



Improving the Achievable Rates of Optical Coherent Transmission with Back-Propagation

Downloaded from: <https://research.chalmers.se>, 2026-04-06 06:46 UTC

Citation for the original published paper (version of record):

Rabbani, H., Rabbani, H., Beygi, L. et al (2018). Improving the Achievable Rates of Optical Coherent Transmission with Back-Propagation. *IEEE Photonics Technology Letters*, 30(14): 1273-1276. <http://dx.doi.org/10.1109/LPT.2018.2839652>

N.B. When citing this work, cite the original published paper.

© 2018 IEEE. Personal use of this material is permitted. Permission from IEEE must be obtained for all other uses, in any current or future media, including reprinting/republishing this material for advertising or promotional purposes, or reuse of any copyrighted component of this work in other works.

Improving the Achievable Rates of Optical Coherent Transmission with Back-Propagation

Hami Rabbani, Hamed Rabbani, Lotfollah Beygi, and Erik Agrell

Abstract—The power allocation in wavelength-division multiplexed (WDM) fiber-optic links with digital back-propagation is optimized in order to improve the achievable rates (AR). The power allocation is performed using a convex optimization technique based on a modulation-format-dependent time-domain model capable of including the nonlinear Kerr effects. In a fully loaded WDM link with heterogeneous (uneven) nonlinear interference noise (NLIN) spectrum, the AR gain of nonlinear back-propagation (BP) over linear electronic dispersion compensation is 60 % larger if per-channel power optimization is allowed than if all transceivers use an equal (flat) optimized power. The heterogeneous NLIN spectrum results from performing BP on a subset of the channels. However, the gain of per-channel power optimization disappears for the homogeneous (nearly flat) NLIN spectrum. Moreover, we show that the improvement obtained by joint channel power allocation is more pronounced for links with a larger number of spans.

Index Terms—Optical coherent communications, Gaussian noise nonlinear model, digital back-propagation, time-domain nonlinear noise model, convex power optimization.

I. INTRODUCTION

A VARIETY of studies have been focused on the possibility that the Kerr-effect nonlinearity can impose a finite limit to the fiber-optic channel capacity [1]. Achievable rates (AR) in fiber-optic transmission have been obtained by exploiting digital back-propagation (BP) [2] to cope with nonlinear effects, described by the nonlinear Schrödinger equation. Low-complexity versions of the BP method were described in [3]. A detailed numerical study of the AR performance for high spectral efficiency long-haul optical communication systems was presented in [4] employing pragmatic decoders and equalization schemes, including electronic dispersion compensation (EDC) and BP.

As digital signal processing technology becomes faster and less costly, EDC is gradually being replaced with BP in optical networks. The transition goes slowly, however, and in the foreseeable future, long-haul networks will involve a combination of EDC and BP in different parts of the network, or different wavelength ranges [3]. Even multichannel BP, which is significantly more complex than single-channel BP, is being considered to an increasing degree [5], [6]. Furthermore, applying multichannel BP over a subset of the C-band enables the compensation of wavelength-dependent fiber parameters.

Hami Rabbani and Lotfollah Beygi are with the EE Dept. of K. N. Toosi University of Technology, Iran. Hamed Rabbani is with the Huawei Technology Company, Iran. Erik Agrell is with the Dept. of Electrical Engineering, Chalmers University of Technology, Sweden. E-mail: hami.rabbani@email.kntu.ac.ir, hamedrabbani@stu.yazd.ac.ir, beygi@kntu.ac.ir, and agrell@chalmers.se.

The importance of channel models in nonlinearity mitigation, especially the Gaussian assumption, was studied and used to devise improved detection strategies [7]. Nonlinear compensation based on BP was used in several works such as [6], [8] to evaluate AR lower bound of a fully-loaded wavelength-division multiplexed (WDM) link. To this end, an equal (flat) launch power in all WDM channels was considered [6]. It was optimized to maximize the signal-to-noise ratio (SNR) of the center channel by taking into account nonlinear signal–signal and signal–noise interactions based on the above mentioned time-domain model [9], [10]. In order to maximize the BP performance of hybrid modulation optical systems, optimization of the power-ratio between modulation formats optical channels was investigated in [11] experimentally.

In this work, we investigate the AR of a back-propagated dense WDM link by performing joint WDM channel power optimization, assuming that the accumulation of amplified spontaneous emission (ASE) noise and nonlinear interference noise (NLIN) is approximated by additive white Gaussian noise at the receiver, based on the modulation-format-dependent time-domain model introduced in [10]. In contrast to previous work [6], we assume that all the WDM channels can have different launch powers, but these channels are considered to have the same source and destination. Then, we optimize the launch power of the WDM channels jointly using an analytic convex mathematical formulation (similar to the approach introduced in [12] for the Gaussian noise (GN) model) to improve the total AR over all WDM channels. We show that the total AR improvement obtained by BP compared with EDC is more than 60 % if a joint power optimization (with different per-channel power) is allowed than if all transceivers use an optimized flat (equal) launch power, provided that the NLIN spectrum is heterogeneous or uneven.

II. SYSTEM MODEL AND OPTIMIZATION FORMULATION

The nonlinear interaction among WDM channels can be categorized as self-channel interference (SCI), cross-channel interference (XCI), and multichannel interference (MCI) including four-wave mixing. In this work, we ignore MCI, as the walk-off effect is large enough in the assumed pseudo-linear working regime [9] to cancel the nonlinear interference effect of the MCI terms. We notice here that this assumption may not be valid for multi-carrier modulation. The SCI and some of the XCI effects can be effectively canceled by multichannel BP, but this technique incurs a high computational complexity and requires a high sampling rate due to the large signal bandwidth. Therefore, considering a WDM system with N channels,

the BP method is performed over only $N_{\text{BP}} < N$ adjacent channels. These channels are $k = \Delta_{\text{BP}} + 1, \dots, \Delta_{\text{BP}} + N_{\text{BP}}$, where Δ_{BP} denotes the offset of the selected N_{BP} channels among the N WDM channels. For any such channel k , the BP method is performed over a window \mathcal{W}_k consisting of the N_w channels closest to k among the available N channels, as depicted in Fig. 1. The left subfigure shows the case when the selected N_{BP} channels are located at the edge of the spectrum ($\Delta_{\text{BP}} = 0$) and the right when they are not ($\Delta_{\text{BP}} > 0$). The remaining $N - N_{\text{BP}}$ channels are solely compensated using linear EDC. In addition, to make a well formulated convex optimization problem, ideal back-propagation within the chosen window helps to simplify the analysis. As a future work, we may consider to study power optimization using suboptimal nonlinear compensation techniques [3] with lower complexity or mitigate the complexity of multi-channel BP by exploiting block-based approaches instead of the introduced sliding-window approach.

The time-domain model in [10] is exploited to evaluate the SNR of a multichannel WDM transmission fiber-optic link with BP. As in [6], all signal–noise and noise–noise nonlinear interactions within the BP window are neglected. Thus, the NLIN power of channel k is

$$P_{\text{NLIN}_k} = \sum_{j=1, j \notin \mathcal{W}_k}^N p_k p_j^2 \chi_{j,k}, \quad (1)$$

where p_j is the launch power of channel j and

$$\chi_{j,k} = \frac{8}{27} \chi_1^{j,k} + \frac{20}{81} \left[\left(\frac{\mathbb{E}\{|B_j|^4\}}{\mathbb{E}^2\{|B_j|^2\}} - 2 \right) \chi_2^{j,k} \right], \quad (2)$$

in which $\chi_1^{j,k}$ and $\chi_2^{j,k}$ are calculated by first replacing q in [10, Eq. (18)] with $|j-k|q$ and then using [10, Eqs. (26–27)]. Here, \mathbb{E} denotes the expectation operator and B_j denotes the random symbol transmitted over interfering channel j . As mentioned, SCI is assumed to be completely canceled by the BP method. Therefore, the SNR of the back-propagated channel k can be written as

$$\text{SNR}_k = \frac{p_k}{\sigma_{\text{ASE}}^2 + P_{\text{NLIN}_k}}, \quad (3)$$

where σ_{ASE}^2 is the ASE noise power.

The NLIN power of channel k with only EDC is

$$P'_{\text{NLIN}_k} = \sigma_{\text{SCI}_k}^2 + \sum_{j=1, j \neq k}^N p_k p_j^2 \chi_{j,k}, \quad (4)$$

in analogy with [12, Eq. (2)] for the GN model, where the SCI power $\sigma_{\text{SCI}_k}^2$ is computed by [13, Eqs. (5)–(9)]. The SNR of this channel, including SCI and XCI but not MCI, is

$$\text{SNR}_k = \frac{p_k}{\sigma_{\text{ASE}}^2 + P'_{\text{NLIN}_k}}, \quad (5)$$

Although in general the probability distribution function of the NLIN converges to a noncircular Gaussian distribution [9], it is approximated here with a circularly symmetric Gaussian distribution. Considering a discrete-time channel model with additive white Gaussian noise and mismatched decoding (treating interference as noise) [1], the AR lower bound of a dual-

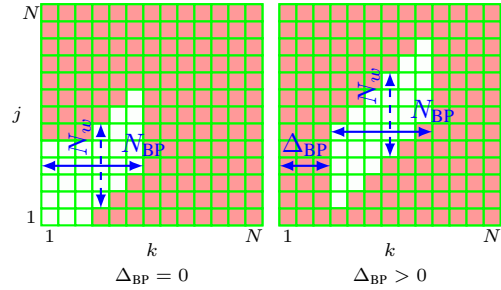


Figure 1. The spectrum of a WDM fiber-optic link with a BP window size of N_w over each of N_{BP} channels. The BP channels are selected contiguously among the available N channels with an offset of Δ_{BP} channels from the lower spectrum edge.

polarized WDM link in bits per channel use is

$$R = 2 \sum_{k=1}^N \log_2(1 + \text{SNR}_k), \quad (6)$$

where SNR_k is given by (3) if $\Delta_{\text{BP}} + 1 \leq k \leq \Delta_{\text{BP}} + N_{\text{BP}}$ and by (5) otherwise.

Since P_{NLIN_k} and P'_{NLIN_k} are posynomial functions and non-convex in their natural form, the variable change of p_i to e^{y_i} transforms them to a convex function of this new variable, $\mathbf{y} = [y_1, y_2, \dots, y_n]$ [12], [14]. Therefore, (3) and (5) are log-concave, and hence the AR in (6) is also concave in the logarithmic power variable \mathbf{y} . Finally, considering the log-concavity of SNR in \mathbf{y} and using the approximation $\text{SNR} + 1 \approx \text{SNR}$ for high SNRs, although the log-concavity is not closed under addition, the AR can be assumed locally concave. Hence, the AR of a WDM link can be maximized with a numerical gradient ascent optimization method, provided that a reasonable initial power vector is chosen [12], [14]. In the following, the AR (6) with and without BP is maximized, considering the following three scenarios.

1) *EDC*: The case without BP, performing only linear EDC for all WDM channels and assuming a constant (flat) power for all channels, serves as a benchmark. The AR is evaluated by (6) with $N_{\text{BP}} = 0$ and a constant launch power $p_1 = \dots = p_N$. The maximum AR obtained by optimizing this power is denoted by $R_{\text{EDC}}^{\text{flat}}$.

2) *BP with flat launch power optimization*: All WDM channels are considered to have a constant launch power $p_1 = \dots = p_N$. This single power is computed such that (6) is maximized, and the obtained AR is denoted by $R_{\text{BP}}^{\text{flat}}$.

3) *BP with N -dimensional launch power optimization*: The AR in (6) is maximized with individual (different) power values p_1, \dots, p_N for the WDM channels by solving an N -dimensional optimization problem. The obtained AR is denoted by $R_{\text{BP}}^{\text{opt}}$.

III. NUMERICAL RESULTS AND DISCUSSION

A dual-polarized coherent transmission link consisting of 100 km spans of a standard single-mode fiber was simulated. The following parameters were used: Dispersion coefficient 17 ps/(nm-km), nonlinear coefficient $1.3 \text{ W}^{-1}\text{km}^{-1}$, attenuation 0.2 dB/km, EDFA noise figure 5 dB, optical center

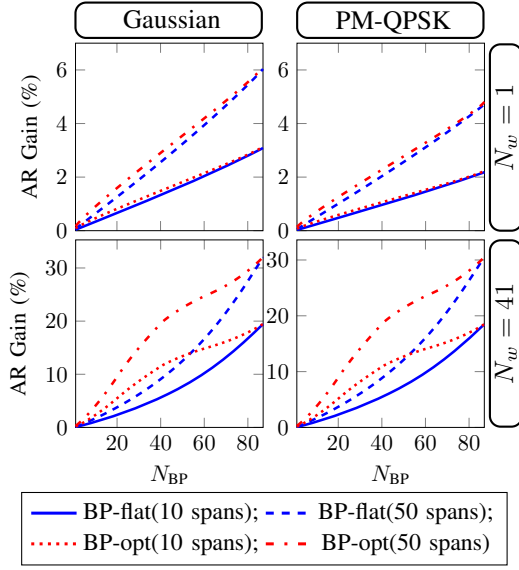


Figure 2. AR gains versus N_{BP} for $N_w = 1$ and 41. Solid and dashed curves show $R_{BP}^{flat}/R_{EDC}^{flat} - 1$, whereas dotted and dash-dotted curves show $R_{BP}^{opt}/R_{EDC}^{flat} - 1$.

wavelength 1550 nm, and symbol rate 32 Gbaud. The pulse shape was raised cosine with a roll-off factor of 0.01 and two modulation formats, Gaussian and polarization multiplexed quadrature phase shift keying (PM-QPSK). We elaborate on the effects of joint BP and power optimization on the AR gain of a fully-utilized simulated WDM link, accommodating $N = 87$ channels with channel spacing of 50 GHz. Specifically, we analyze the performance of multichannel BP with $N_w = 41$ and more practical single-channel BP, i.e., $N_w = 1$, with lower computational complexity.

A. $\Delta_{BP} = 0$

In Fig. 2, the AR gain of BP over EDC is shown as a function of N_{BP} for $N_w = 1$ and 41, with flat (equal) and per-channel power optimization. For $N_w = 1$, the AR gain of per-channel compared to flat optimization is not considerable due to the homogeneous NLIN spectrum, as observed also in [12]. In fact, the role of per-channel power optimization is more highlighted for $N_w = 41$ especially for N_{BP} values in the range of 20–60, resulting from the heterogeneous NLIN spectrum. This gain improvement disappears for small and large N_{BP} values. In the other extreme, $N_w = 86$ (not shown), the AR gains behave similarly as in Fig. 2 with $N_w = 41$. The AR gain by N -dimensional power optimization over flat power optimization, i.e., $R_{BP}^{opt}/R_{BP}^{flat} - 1$, is demonstrated in Fig. 3 as a function of N_w and the number of spans in the link. As seen, this gain is more prominent for increasing N_w . Furthermore, Figs. 2 and 3 indicate that the gain is higher for a larger number of spans. As seen in Figs. 2 and 3, the AR gain of Gaussian modulation is higher than PM-QPSK, since the PM-QPSK modulation maximizes the modulation format-dependent correction terms.

Fig. 4 shows the optimized launch power vector of WDM channels and their corresponding SNR values, obtained by N -dimensional power optimization for a link with 10 and 50

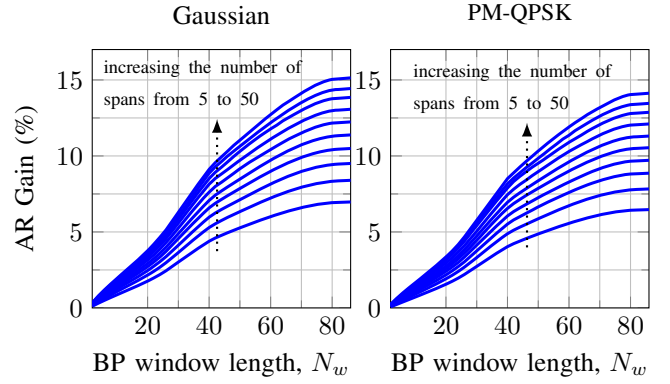


Figure 3. AR gain $R_{BP}^{opt}/R_{BP}^{flat} - 1$ versus N_w for $0 < N_w < 87$ and $N_{BP} = 40$.

spans. As seen in this figure, the optimized launch power values of N_{BP} back-propagated channels are higher than the channels with only EDC. This is explained by the quadratic growth of NLIN with the launch power for the channels with BP, compared to its cubic growth for channels with EDC [15]. Moreover, the low-pass behavior of XCI effect results in allocating the highest power value to the channel located at the edge of spectrum for $N_w = 1$. The highest power is allocated to a channel located $N_{BP}/2$ channels away from (to the left of) the last back-propagated channel for $N_w = 41$. The SNR values of WDM channels in the second row of Fig. 4 indicate imbalance performance results among back-propagated channels.

B. $\Delta_{BP} > 0$

We next investigate how the total link AR is influenced by shifting the block of N_{BP} back-propagated channels across the spectrum. To this end, we slide $N_{BP} = 40$ channels across the whole spectrum, letting Δ_{BP} go from 0 to $N - N_{BP}$. Figs. 5, first column, show the AR gain of BP with N -dimensional power optimization over EDC with flat power optimization, i.e., $R_{BP}^{opt}/R_{EDC}^{flat} - 1$. Figs. 5, second column, show the AR gain of BP over EDC, both with flat power optimization, i.e., $R_{BP}^{flat}/R_{EDC}^{flat} - 1$. The figures show that the gain of N -dimensional power optimization is higher when the selected N_{BP} channels are closer to the edge of the spectrum than near its center, while the gain of flat launch power optimization with BP is almost constant across the whole spectrum. Furthermore, the AR gains with BP and N -dimensional power optimization (i.e., $R_{BP}^{opt}/R_{EDC}^{flat} - 1$) is more than 1.6 times the gain obtained by BP and flat power optimization (i.e., $R_{BP}^{flat}/R_{EDC}^{flat} - 1$) for $N_w = 41$, while this gap disappears for $N_w = 1$. For $N_w = 86$ (not shown), the behavior of AR gains are in analogy with $N_w = 41$ in Fig. 5. These figures also indicate that if the system designer can choose Δ_{BP} freely for optimum performance, the selected N_{BP} channels should be located close to the edge of spectrum. Finally, as indicated in Figs. 2, 3, and 5, the AR gain with optimized power allocation is improved as the numbers of link spans increases, because the NLIN accumulates coherently across the spans.

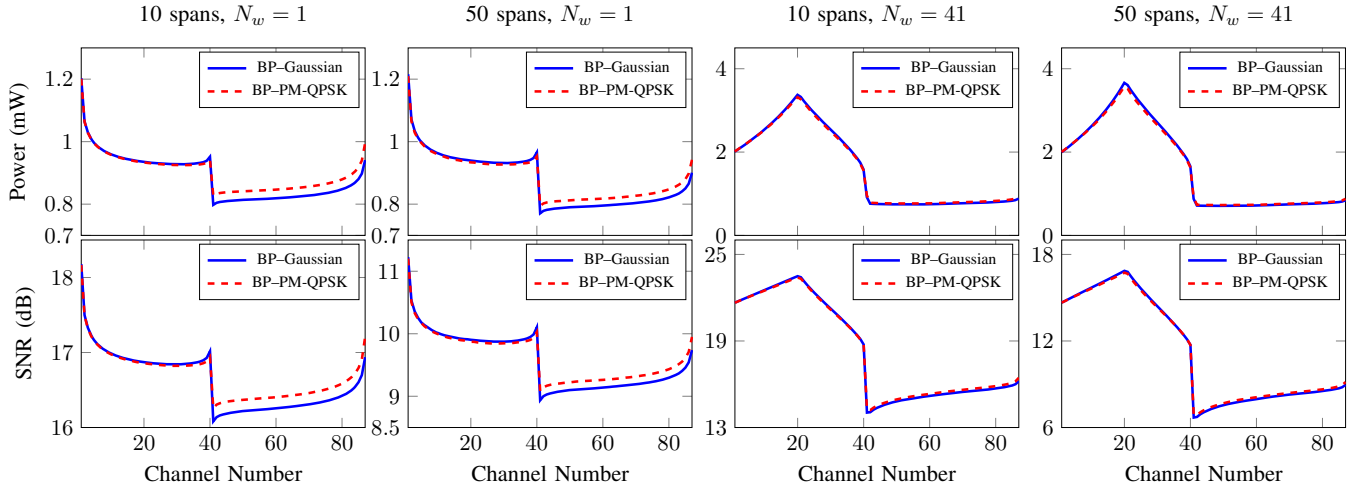


Figure 4. The optimized power values of 87 WDM channels for $N_w = 1$ and 41 are shown in the first row with the corresponding SNR values in the second row. The $N_{BP} = 40$ back-propagated channels are located at the edge of the spectrum.

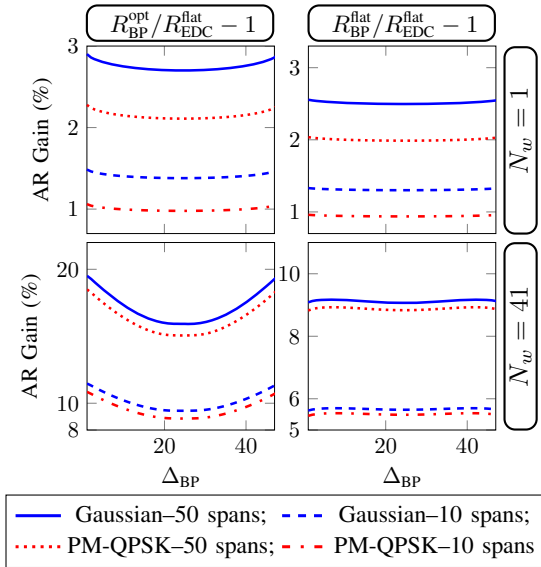


Figure 5. AR gains ($R_{BP}^{opt}/R_{EDC}^{flat} - 1$ in the first column and $R_{BP}^{flat}/R_{EDC}^{flat} - 1$ in the second column) versus Δ_{BP} ($N_{BP} = 40$).

IV. CONCLUSIONS

ARs of a fiber-optic WDM link with fully utilized spectrum was investigated using a time-domain channel model, capable of including the effect of nonlinear interference and its dependence on the modulation format, but neglecting signal-noise interaction. To optimize the AR with BP, two power allocation strategies were studied: Multidimensional launch power optimization and a single, flat power optimization. In both methods, a mathematical convex formulation was introduced to optimize the total link AR. The per-channel compared to single flat power optimization is more effective for large BP window lengths, showing almost no gain for single-channel BP. It was shown that if BP can only be applied to a subset of the WDM channels for complexity reasons, then the back-propagated channels should be located close to the

edge of the spectrum. Finally, the AR gains of BP compared with using EDC on all channels are more pronounced for links with a larger number of spans. The obtained results are valid for systems with large enough accumulated dispersion and may not be applicable in multi-carrier modulation scenarios.

REFERENCES

- [1] M. Secondini *et al.*, "Scope and limitations of the nonlinear Shannon limit," *J. Lightw. Technol.*, vol. 35, no. 4, pp. 893–902, Apr. 2017.
- [2] E. Ip and J. M. Kahn, "Compensation of dispersion and nonlinear impairments using digital backpropagation," *J. Lightw. Technol.*, vol. 26, no. 20, pp. 3416–3425, Oct. 2008.
- [3] D. Rafique, "Fiber nonlinearity compensation: Commercial Applications and Complexity Analysis," *J. Lightw. Technol.*, vol. 34, no. 2, pp. 544–553, Jan. 2016.
- [4] G. Liga *et al.*, "Information rates of next-generation long-haul optical fiber systems using coded modulation," *J. Lightw. Technol.*, vol. 35, no. 1, pp. 113–123, Jan. 2017.
- [5] L. Galdino *et al.*, "On the limits of digital back-propagation in the presence of transceiver noise," *Opt. Express*, vol. 25, no. 4, pp. 4564–4578, Feb. 2017.
- [6] R. Dar and P. J. Winzer, "On the limits of digital back-propagation in fully loaded WDM systems," *IEEE Photon. Technol. Lett.*, vol. 28, no. 11, pp. 1253–1256, Jun. 2016.
- [7] M. Secondini *et al.*, "Fiber nonlinearity mitigation in WDM systems: Strategies and achievable rates," in *Proc. European Conf. and Exhibition on Optic. Commun.*, 2017, W.1.D.5.
- [8] T. Tanimura *et al.*, "Analytical results on back propagation nonlinear compensator with coherent detection," *Opt. Express*, vol. 20, no. 27, pp. 28 779–28 785, Dec. 2012.
- [9] A. Mecozzi and R. J. Essiambre, "Nonlinear Shannon limit in pseudolinear coherent systems," *J. Lightw. Technol.*, vol. 30, no. 12, pp. 2011–2024, Jun. 2012.
- [10] R. Dar *et al.*, "Properties of nonlinear noise in long, dispersion-uncompensated fiber links," *Opt. Express*, vol. 21, no. 22, pp. 25 685–25 699, Nov. 2013.
- [11] S. B. Amado *et al.*, "Nonlinear mitigation of a 400G frequency-hybrid superchannel for the 62.5-GHz slot," *J. Lightw. Technol.*, vol. 35, no. 18, pp. 3963–3973, Sep. 2017.
- [12] I. Roberts, J. M. Kahn, and D. Boertjes, "Convex channel power optimization in nonlinear WDM systems using Gaussian noise model," *J. Lightw. Technol.*, vol. 34, no. 13, pp. 3212–3222, Jul. 2016.
- [13] A. Carena *et al.*, "EGN model of non-linear fiber propagation," *Opt. Express*, vol. 22, no. 13, pp. 16 335–16 362, Jun. 2014.
- [14] S. Boyd and L. Vandenberghe, *Convex Optimization*. Cambridge University Press, 2004.
- [15] L. Beygi *et al.*, "On nonlinearly-induced noise in optical links with digital backpropagation," *Opt. Express*, Nov. 2013.